Molecular analysis of the HPJ-JT syndrome and sporadic parathyroid carcinogenesis

Haven, C.J.

Chapter 2

A genotypic and histopathological study of a large Dutch kindred with hyperparathyroidism-jaw tumor syndrome.

J Clin Endocrinol Metab. 2000 Apr;85(4):1449-54.

0021-972X/00/$03.00/0
The Journal of Clinical Endocrinology & Metabolism

Vol. 85, No. 4
Printed in U.S.A.

A Genotypic and Histopathological Study of a Large Dutch Kindred with Hyperparathyroidism-Jaw Tumor Syndrome*

CAROLA JOSE HAVEN, FUNG KI WONG, EVELINE W. C. M. VAN DAM, ROB VAN DER LUIJT, CHRISTI VAN ASPEREN, JOKE JANSEN, CARLA ROSENBERG, MIREILLE DE WIT, JANINE ROIJERS, JO HOPPENER, CORNELIS J. LIPS, CATHARINA LARSSON, BIN TEAN TEH, AND HANS MORREAU

Department of Pathology (C.J.H., H.M.), Department of Endocrinology (E.W.C.M.v.D.), Department of Clinical Genetics (C.v.A.), Department of Anthropogenetics (C.R.), Leiden University Medical Center, 2300 RC Leiden, The Netherlands; Department of Molecular Medicine (F.K.W., C.L.), Karolinska Hospital, Stockholm, S-17176 Sweden; Department of Medical Genetics (R.v.d.L., M.d.W.), Department of Internal Medicine (J.J., C.J.L.), Department of Internal Medicine and Pathology (J.R., J.H.), University Medical Center Utrecht, 3500 AB Utrecht, The Netherlands; and VanAndel Research Institute (B.T.T.), Grand Rapids, Michigan 49503

ABSTRACT

Familial primary hyperparathyroidism is the main feature of 2 familial endocrine neoplasia syndromes: multiple endocrine neoplasia type 1 (MEN 1) and hyperparathyroidism-jaw tumor syndrome (HPT-JT). The latter is a recently described syndrome that has been associated with ossifying fibroma of the jaw and various types of renal lesions, including benign cysts, Wilms' tumor, and hamartomas. To further illustrate the natural history of this syndrome, we describe a large, previously unreported Dutch kindred in which 13 affected members presented with either parathyroid adenoma or carcinoma; in 5 affected individuals, cystic kidney disease was found. Additionally, pancreatic adenocarcinoma, renal cortical adenoma, papillary renal cell carcinoma, testicular mixed germcell tumor with major seminoma component, and Hürthle cell thyroid adenoma were also identified. Linkage analysis of the family using *MEN1*-linked microsatellite markers and mutation analysis excluded the involvement of the *MEN1* gene. Using markers from the *HPT-JT* region in 1q25–31, cosegregation with the disease was found, with a maximum logarithm of odds score of 2.41 obtained for 6 markers using the most conservative calculation. Meiotic telomeric recombination between D1S413 and D1S477 was identified in 3 affected individuals, and when combined with previous reports, delineated the *HPT-JT* region to 14 centimorgan. Combined comparative genomic hybridization and loss of heterozygosity data revealed complex genetic abnormalities in the tumors, suggesting different possible genetic mechanisms for the disease.

In conclusion, we report a family with hyperparathyroidism linked to chromosome 1q, and exhibiting several types of renal and endocrine tumors that have not been previously described. (*J Clin Endocrinol Metab* **85:** 1449–1454, 2000)

FAMILIAL PRIMARY hyperparathyroidism (HPT) occurs in the context of familial isolated hyperparathyroidism or in families in which a hereditary tumor syndrome is coupled with primary hyperparathyroidism (1). In multiple endocrine neoplasia type 1 (MEN 1), primary hyperparathyroidism is associated with additional endocrine tumors of, *e.g.* pancreas, anterior pituitary, and stomach (2). The disease is associated with mutations inactivating the tumor suppressor gene *MEN1*, located on chromosome (chr.) 11q13 (3, 4). In MEN 2a hyperparathyroidism may occur together with medullary carcinoma of the thyroid or pheochromocytoma caused by germ-line activating mutations of the *RET* protooncogene on chr. 10q11 (5).

A distinct disorder, hereditary hyperparathyroidism-jaw tumor syndrome (HPT-JT), with an autosomal dominant mode of inheritance, has been described in which primary hyperparathyroidism caused by parathyroid adenoma is associated with ossifying fibroma of the jaw (6). In a number of families, parathyroid carcinoma has been noted (7–12). In addition, renal disease has also been described, including renal hamartomas, Wilms' tumor, polycystic kidney disease, and degenerative cysts (8, 11–14). The HPT-JT gene (*HRPT2*) has been mapped to the long arm of chr. 1q25-q31, later narrowed down to a 14.7-cm (centimorgan) region. Additionally, a 0.7-cm candidate region was recently suggested, based on shared haplotypes found in two Northern American families (15).

The nature of the *HRPT2* gene is still unresolved, although [based on the presence or loss of the wild-type alleles in several renal hamartomas and some parathyroid tumors (13, 16)] the *HRPT2* gene is considered a putative tumor suppressor gene. However, loss of heterozygosity (LOH) in HPT-JT is not always as evident as in MEN 1, in which the majority of familial tumors show loss at 11q13. For example, LOH has only been demonstrated in parathyroid tumors from a subset of families (11, 13, 14), possibly suggesting an alternative mechanism for tumorigenesis of parathyroid tu-

Received July 30, 1999. Revision received November 8, 1999. Accepted December 20, 1999.

Address correspondence and requests for reprints to: Dr. Hans Morreau, Department of Pathology, Leiden University Medical Center, P.O. Box 9600, L1-Q, Building I, 2300 RC Leiden, The Netherlands. E-mail: jmorreau@pat.azl.nl.

* This study was supported by the Swedish Cancer Foundation, Torsten and Ragnar Söderberg Foundation, and Gustav V Jubilee Fund.

mors in HPT-JT patients. To further understand the natural history and genetic involvement of this relatively new syndrome, we have studied the clinical, histopathological, and genotypic characteristics of a large Dutch kindred in which primary hyperparathyroidism is associated with other neoplasia.

Subjects and Methods

The pedigree of the family with the clinical phenotypes is shown in Fig. 1. To date, 13 family members have been documented with primary hyperparathyroidism caused by parathyroid adenoma. Five individuals (III-2, III-5, III-8, III-10, and III-11) had multiple renal cysts. Four of them (III-2, III-5, III-10, and III-11) developed renal insufficiency requiring dialysis. The sex distribution of affected individuals is roughly equal.

Additional tumors were found in four patients. These were Hürthle cell adenoma of the thyroid gland with cystic changes (III-2 at age 44), clear cell adenocarcinoma of the pancreas (III-2 at age 48, Fig. 2), papillary renal cell carcinoma and multiple cortical renal cell adenomas in the right kidney (III-5 at age 54, Fig. 2), parathyroid adenoma with atypia (III-11 at age 32) and parathyroid carcinoma (III-11 at age 36, Fig. 2), and left testicular mixed germcell tumor with a major seminoma component (IV-4 at age 32). Clinically unaffected carriers with the disease haplotype that were screened by renal ultrasonography (III-21, IV-7, IV-9, IV-12, and IV-13) showed no apparent abnormalities. Also the renal ultrasonography of carriers IV-11 and IV-14 was normal. Current biochemical testing of Ca^{2+} and PTH of individuals III-4, III-21, IV-7, IV-8, IV-9, IV-11, IV-12, IV-13, and IV-14 was normal. Of the four individuals (IV-11, IV-12, IV-13, and IV-14) that were radiographically screened, only two (IV-13 and IV-14) were suspect for carrying a small jaw tumor; however, this has not been histologically documented.

Linkage analysis

Informed consent was obtained from all participating members of the family or their legal representatives.

High-molecular-weight DNA was isolated from leukocytes using standard methods. For two patients (III-2 and III-11) from whom a blood sample could not be obtained, constitutional DNA was extracted from nontumorous formalin-fixed paraffin-embedded tissue, as described (17). Eight microsatellite markers in and flanking the *MEN1* gene in 11q13, cen-D11S4945-PYGM-D11S4946-D11S4940-D11S4947-D11S1783-D11S4937-D11S4936-tel, were used (4, 18). The 3–7th markers mentioned are intragenic, the other three are flanking the *MEN1* locus. Eleven microsatellite markers from a 26-cm region in 1q25-q31, between D1S215 and D1S249, encompassing the *HPRT2* locus (12), cen D1S215, D1S466, D1S191, D1S254, D1S422, D1S428, D1S222, D1S412, D1S413, D1S477, D1S510 (Genome Database: www. gdb.org) were used for linkage.

Genotyping was carried out by two methods: one using radiolabeled markers and the other fluorescent markers. PCR reactions were performed in a total vol of 10 μl, containing 100 ng genomic tumor DNA, 50 mmol/L KCL, 10 mmol/L Tris-HCL (pH 8.3), 1,5 mmol/L MgCl2, 125 mmol/L of each deoxynucleotide triphosphate, 2 pmol of each oligodeoxynucleotide primer (one of which was end-labeled with ^{32}Phosphate in the case of radiolabeled markers), and 0.2 U DNA C polymerase (Dynazyme/*Taq* polymerase). Samples were amplified for 30 cycles (denaturation at 96 C for 30 sec, annealing at 55 C for 30 sec, and elongation at 72 C for 30 sec; and the products were run on 1% polyacrylamide gels.

With the fluorescent markers, the PCR products were pooled into three panels, according to the emission spectra of fluorescent dyes and the expected sizes of the amplified products. Electrophoresis was performed on 6% polyacrylamide gels, running on an ABI 377 laser-fluorescent sequencer (Perkin-Elmer Corp., Foster City, CA), and electrophoresis data were analyzed with the Genescan 3.1 computer software (Perkin-Elmer Corp.).

Two point logarithm of odds (lod) scores were generated using the LINKAGE (version 5.1) program adopting a conservative approach. Only patients with primary HPT were scored as affected, whereas other members at risk were considered as unknown. An autosomal dominant mode of inheritance and a penetrance of 0.90 were assumed.

Tumor analysis

Formalin-fixed, paraffin-embedded tumor tissue was obtained from 4 patients (III-2, III-5, III-11, and IV-1) and fresh frozen tumor tissue samples from 2 other patients (IV-11 and IV-14). Whenever possible, different tumor foci, as selected by a pathologist (H. Morreau), were microdissected from 10 10-μm-thick hematoxylin-stained sections

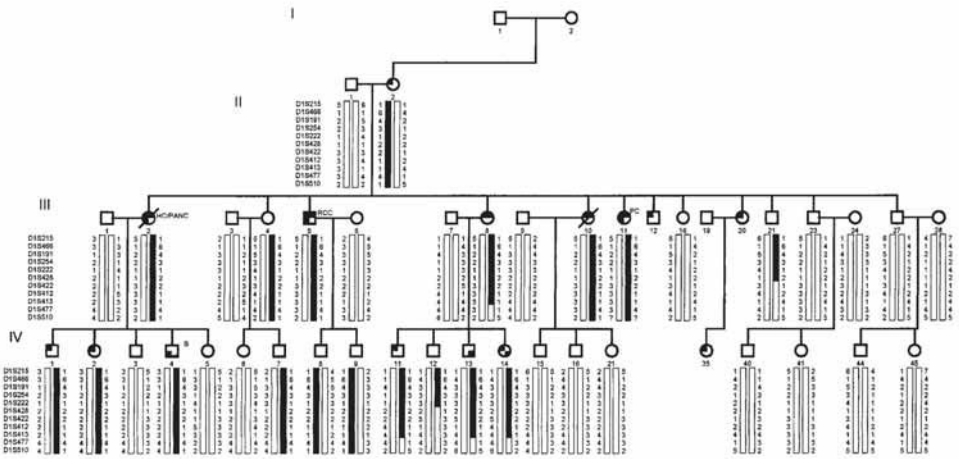

FIG. 1. Pedigrees and phenotypes of the family in this study. ◔, ◨, Hyperparathyroidism; ◔, ◨, renal cysts, ◶, ◪, jaw tumor; ○, □, unaffected; ◶, ◪, additional neoplasm; S, mixed germcell tumor with major seminoma component; RCC, renal cell carcinoma; PC, parathyroid carcinoma; HC, Hürthle cell adenoma of the thyroid. The affected haplotype is indicated by *black bars*.

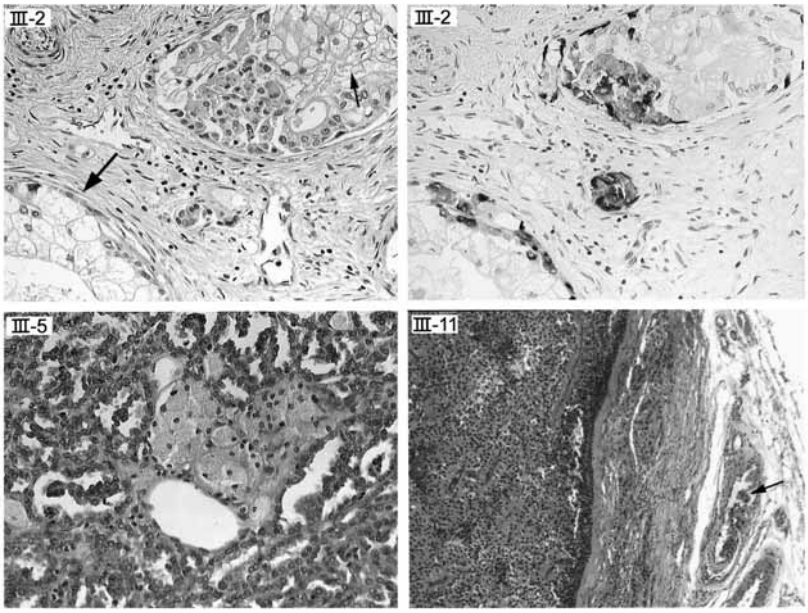

FIG. 2. Light microscopic pictures of three different tumors from individuals III-2, III-5, and III-11. III-2, a glandular area of the clear-cell adenocarcinoma of the pancreas (*top left*, *thick arrow*) is shown. In the surrounding preexistent pancreatic tissue, atypical ductal hyperplasia was present. Clear cells, similar to the infiltrating carcinoma cells, can be seen in islets of Langerhans (*top left*, *small arrow*). Positive staining with antibodies against neuron-specific enolase (NSE) is shown, indicating neuroendocrine features (*top right*). The islets stain positive also with antibodies against insulin and glucagon (data not shown). *Bottom left*, the papillary renal cell carcinoma from individual III-5 is shown; *bottom right*, the parathyroid carcinoma from individual III-11. The *arrow* indicates vasoinvasive growth of tumor cells.

mounted on glass-slides. Genomic DNA was extracted from the paraffin-embedded and fresh frozen specimens using standard methods.

Matched pairs of constitutional and tumor DNA were genotyped and analyzed for allelic imbalance, using markers as described under linkage analysis. For the chr.1q region, additional markers D1S2125, D1S1653, D1S408, D1S1614, D1S533, and D1S1660 were used. Allele status was identified on autoradiographic films and confirmed by digital images, which permitted computerized calculations of relative allele intensities. LOH was considered present when the signal intensity of one allele was reduced by more than 50%, in comparison with the corresponding allele in normal DNA.

Comparative genomic hybridization (CGH)

DNA from tumor samples was labeled with Fluorescein-12-deoxyuridine 5-triphosphate and DNA from the normal control with Lissamine-5-deoxyuridine 5-triphosphate (both from NEN Life Science Products, Boston, MA) by standard nick-translation.

The CGH was then performed according to the protocol described by Kallioniemi *et al.*(19), with a few modifications. Briefly, 200 ng of each labeled tumor and control DNA and 10 μg of human Cot-1 DNA (Life Technologies/BRL, Gaithersburg, MD) were dissolved in 10 μl hybridization buffer (50% formamide/2 $\times$ SSC/10% dextran-sulphate) and hybridized to normal male metaphase spreads at 37 C for 4 days. Post-hybridization washes were performed with 2 $\times$ SSC at 37 C (3 $\times$ 10 min) followed by 0.1 $\times$ SSC at 60 C (3 $\times$ 5 min). Chromosomes were counterstained with 4,6-diamidino-2-phenylindole (0.5 μg/mL) in Vectashield antifade solution (Vector Laboratories, Inc., Burlingame, CA). Images were captured with a DM microscope (Leica Corp., Heidelberg, Germany) equipped with three single excitation filters, a multi-bandpass dichroic mirror, a multiband pass emission filter (P-1 filter set; Chroma Technology, Brattleborough, VT), and a cooled CCD camera (Photometrics Inc., Tucson, AZ). The green, red, and blue images were collected sequentially by changing the excitation filter. Images were analyzed using the QUIPS XL software from Vysis (Downers Grove, IL).

Losses of DNA sequences were defined as chromosomal regions where the average green-to-red ratio and its 95% confidence interval were below 0.8, whereas gains were above 1.2. These threshold values were based on measurements from a series of normal controls

Mutation analysis of the MEN1 gene

Mutation analysis was performed using single-stranded conformational polymorphism analysis and direct sequencing of all 10 exons and flanking intronic sequences after amplification of genomic DNA, as described (20).

Results

No germline mutations in the *MEN1* gene were detected. Furthermore, no linkage could be demonstrated for markers chosen in the 11q13 region. No LOH for markers at 11q13 was identified in eight tumors tested (data not shown).

Analysis of 11 markers indicated that primary HPT in this kindred was linked to the 1q25–31 *HPT-JT* region. The maximum 2-point lod score of 2.41 was obtained with markers

TABLE 1. Lod scores for linkage to chromosome 1q21–q32 markers in the family

Locus	Recombination fraction (θ)					
	0.000	0.010	0.05	0.100	0.200	0.300
D1S215	1.202	1.18	1.091	0.974	0.719	0.438
D1S466	2.405	2.362	2.182	1.948	1.437	0.865
D1S191	2.405	2.362	2.182	1.948	1.437	0.865
D1S254	2.405	2.363	2.182	1.948	1.437	0.865
D1S222	1.202	1.18	1.091	0.974	0.719	0.438
D1S428	1.202	1.18	1.091	0.974	0.719	0.438
D1S422	2.405	2.363	2.182	1.948	1.437	0.865
D1S412	2.405	2.363	2.182	1.948	1.437	0.865
D1S413	2.405	2.363	2.182	1.948	1.437	0.865
D1S477	−5.423	−1.614	−0.370	0.0047	0.245	0.224
D1S510	−5.492	−1.619	−0.372	−0.420	0.245	0.182
428 + 422	2.405	2.362	2.182	1.948	1.437	0.865
412 + 413	2.405	2.362	2.182	1.948	1.437	0.865

TABLE 2. LOH on chromosome 1q in different tumors from obligate gene-carriers

III-2	III-5		III-11		IV-1	IV-11	IV-14	Case no.
Pancreatic carcinoma	Renal cortical adenoma	Papillary renal cell carcinoma	Parathyroid adenoma	Parathyroid carcinoma	Parathyroid adenoma	Parathyroid adenoma	Parathyroid adenoma	pathology
								Locus
LOH	R	R	–	R	R	–	–	D1S2125
LOH	R	R	R	–	R	–	–	D1S1653
–	R	R	R	–	R	–	–	D1S215
–	–	–	–	–	–	R	R	D1S254
LOH	–	–	–	–	–	–	–	D1S428
LOH	R	R	–	–	–	R	R	D1S422
LOH	R	LOH d	R	R	–	R	R	D1S408
LOH	–	–	–	LOH w	R	R	R	D1S412
LOH	–	–	R	LOH d	R	R	R	D1S1614
–	–	–	–	–	R	R	R	D1S533
LOH	–	–	–	–	R	R	R	D1S413
–	–	–	–	–	R	R	R	D1S1660
–	–	–	–	–	–	–	–	D1S477
–	–	–	–	–	–	–	–	D1S510

R, Retention; w, wild-type allele; d, defective allele; –, not informative.

D1S466, D1S191, D1S254, D1S422, D1S412, and D1S413 (Table 1). Considering that the most conservative approach was used in our calculation, *i.e.* all individuals at risk were labeled as unknown, the lod score obtained is the maximum possible in this family. All affected individuals carried the disease haplotype (Fig. 1).

Meiotic recombination of the mutated chromosome was seen in patient III-8 (between D1S413 and D1S477), and the same telomeric recombination was transmitted to her offspring IV-11, IV-13, and IV-14 (Fig. 1). Her clinically unaffected son (IV-12) exhibited a recombination between D1S222 and D1S428. The unaffected male III-21 (at age 50) exhibited a recombination between D1S428 and D1S422.

LOH studies (Table 2) with markers from the HPT-JT genomic region identified no LOH at chr. 1q21–32 in any of the parathyroid adenomas or in a renal cell cortical adenoma studied. Only different foci of the pancreatic adenocarcinoma (III-2), the papillary renal cell carcinoma (III-5), and the parathyroid carcinoma (III-11) exhibited LOH in the chr.1q region, involving either the defective or wild-type chromosome (Table 2). CGH of fresh-frozen tissue from two parathyroid adenomas of the family (IV-11 and IV-14) revealed amplification of chr.16 for the tumor from IV-11 and deletion of chr.13q, as well as amplification of chr.1q and chr.17p for the tumor from IV-14.

Discussion

The familial inheritance of parathyroid adenoma/carcinoma and cystic kidney disease, its genetic exclusion of MEN 1, and the lod score of 2.41 with 6 markers at 1q25–31 strongly point to the diagnosis of HPT-JT syndrome. The latter is relatively new, and the spectrum of its clinical features is far from fully understood, as exemplified in this family. Several types of tumors occurring in this family (including pancreatic adenocarcinoma, renal cortical adenoma, papillary renal cell carcinoma, testicular mixed germcell tumor with major seminoma component, and Hürthle cell thyroid adenoma) have not been previously described in this syndrome. Although coincidence can not be ruled out, their occurrence in affected patients with parathyroid tumors and their multiplicity (*e.g.* renal cortical adenoma) indicate their association with the syndrome. Some of these tumors have been associated with or reported in other familial neoplasia syndromes. For example, papillary renal cell carcinoma is the main feature of hereditary papillary renal carcinoma syndrome involving chr.7; and in one such family, two cases of pancreatic car-

TABLE 3. Diagram illustrating recombination events defining the *HRPT2* region.

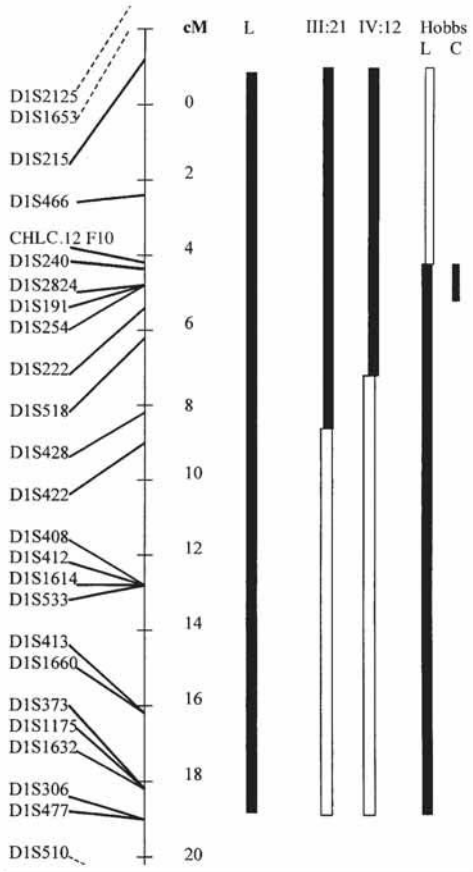

A scale and the approximate locations of markers on chromosome 1q are given on the left. The first vertical bar represents the recombination data of the family obtained by linkage analysis of affected individuals. The second and third bars denote the recombination data of two (yet) clinically unaffected individuals (III-21, IV-12). The fourth and fifth bars illustrate the 14.7 and 0.7 cM proposed candidate region for *HRPT2*, as described by Hobbs *et al.* (15).

cM, Centimorgan; L, linkage data; C, proposed candidate region.

cinoma have been described (21, 22). Of interest is that a subset of papillary renal cell carcinomas is known to carry a t(X;1)(p11;q21) as the sole cytogenetic abnormality present (23, 24). The breakpoint locus at 1q, however, does not seem to be located within the *HRPT2* region. Additionally, renal cortical adenomas have been described in von Hippel-Lindau syndrome (25); and testicular cancer, in familial testicular cancer syndrome (26).

The *HRPT2* region has been narrowed to 14.7 cm by the identification of recombinations in affected cases (15). A 0.7-cm candidate region was proposed, based on shared haplotypes in two Northern American families, but this data warrants confirmation. In the present studies, a number of recombinants have been identified. Three clinically affected cases (III-8, IV-11, and IV-14) carry a telomeric recombination between D1S413 and D1S477 which is the closest telomeric border found in affected cases. Therefore, when combining previously published data, the HPT-JT locus can be delineated to 14 cm bordered by marker CHLC.12F10 (15) and D1S1632 (present study) (Table 3). Interestingly, two critical re-combinants were identified in two members who remain disease-free to date. The first one is in a 50-yr-old man (III-21) who carries a telomeric recombination between markers D1S428 and D1S422, and the second is in a 34-yr-old man (IV-12) with recombination between D1S222 and D1S428. However, reduced penetrance is not uncommon in HPT-JT (9, 11), as evidenced by six other diseased haplotype carriers: III-4 (aged 62), IV-4 (aged 30), IV-7 (aged 24), IV-8 (aged 32), IV-9 (aged 30), and IV-13 (aged 33). As such, we are treating the two disease-free recombinants with great caution, although they may potentially further narrow the region. The *HRPT2* gene has been proposed as a putative tumor suppressor gene based on LOH involving the wild-type alleles in a subset of 1q-linked tumors (11, 13, 16). However, in the present study, we were unable to demonstrate consistent LOH of 1q21–32 in the tumors analyzed. This is in keeping with other published data that indicates that an imbalance at 1q is not always found in HPT-JT-related tumors (13, 14). It may be that the LOH detected in our study on chr.1 is a late somatic event during tumorigenesis, because only the malignant tumors exhibited this pattern. In addition, our CGH results, which showed amplification of chr.1q in one of the two parathyroid adenomas, are consistent with the CGH results of two other 1q-linked parathyroid tumors (16). Taken together, these complex data may suggest a different scenario: the involvement of an oncogene in which loss of the wild-type copy was a secondary event and followed by duplication of the mutated copy. A similar mechanism has been found in hereditary papillary renal cell carcinomas involving the *MET* locus on chr. 7 (21, 22, 27). Finally, the gain at chr. 16q and the loss at chr.13q by CGH analysis in the parathyroid adenomas in our family have also been described by others (16), suggesting a role for these regions in parathyroid tumorigenesis and progression. Future identification of the *HRPT2* gene will lead to a better understanding of the mechanisms causing this interesting disease to have a wide spectrum of clinical features.

Acknowledgments

We thank Dr. Annemarie Cleton and Wiljo de Leeuw for their technical advice, and Klaas van der Ham for excellent photographic work. Prof. Dr. G. J. Fleuren is thanked for his continuous support.

References

1. **Pearce SHS, Thakker RV.** 1997 Molecular genetics of parathyroid disorders. In: Thakker, ed. Molecular genetics of endocrine disorders. Chapman and Hall Medical; 123–152.

2. **Larsson C, Nordenskköld M, Zedenius J.** 1995 Multiple endocrine neoplasia types 1 and 2. In: Cowell JK, ed. Molecular genetics of cancer. BIOS; 71–92.
3. **Larsson C, Skogseid B, Öberg K, Nakamura Y, Nordenskjöld M.** 1988 Multiple endocrine neoplasia type 1 gene maps to chromosome 11 and is lost in insulinoma. Nature 332:85–87.
4. **Chandrasekharappa SC, Guru SC, Manickam P,** et al. 1997 Positional cloning of the gene for multiple endocrine neoplasia-type 1. Science. 276:404–407.
5. **Eng C.** 1999 Ret protooncogene in the development of human cancer. J Clin Oncol. 17:380–393.
6. **Jackson CE, Norum RA, Boyd SB, et al.** 1997 Hereditary hyperparathyroidism and multiple ossifying jaw fibromas: a clinically and genetically distinct syndrome. Hum Genet. 101:102–108.
7. **Dinnen JS, Greenwood RH, Jones JH, Walker DA, Williams ED.** 1977 Parathyroid carcinoma in familial hyperparathyroidism. J Clin Pathol. 30:966–975.
8. **Kakinuma A, Morimoto I, Nakano Y, et al.** 1994 Familial primary hyperparathyroidism complicated with Wilms' tumor. Intern Med. 33:123–126.
9. **Fujikawa M, Okamura K, Sato K, et al.** 1998 Familial isolated hyperparathyroidism due to multiple adenomas associated with ossifying jaw fibroma and multiple uterine adenomyomatous polyps. Eur J Endocrinol.138:557–561.
10. **Pidwirny GN, Szabo J, Hobbs M, Heath H, Jackson CE.** 1995 Follow-up of two hyperparathyroidism-jaw tumors syndrome families reported in 1971 and 1981 reveals that they are related and that parathyroid cancer is a part of the syndrome. Am J Hum Genet. 57:A75.
11. **Teh BT, Farnebo F, Twigg S, et al.** 1998 Familial isolated hyperparathyroidism maps to the hyperparathyroidism-jaw tumor locus in 1q21–q32 in a subset of families. J Clin Endocrinol Metab. 83:2114–2120.
12. **Wassif WS, Farnebo F, Teh BT, et al.** 1999 Genetic studies of a family with hereditary hyperparathyroidism-jaw tumour syndrome. Clin Endocrinol (Oxf). 50:191–196.
13. **Teh BT, Farnebo F, Kristoffersson U, et al.** 1996 Autosomal dominant primary hyperparathyroidism and jaw tumor syndrome associated with renal hamartomas and cystic kidney disease: linkage to 1q21–q32 and loss of the wild-type allele in renal hamartomas. J Clin Endocrinol Metab. 81:4204–4211.
14. **Szabo J, Heath B, Hill VM, et al.** 1995 Hereditary hyperparathyroidism-jaw tumor syndrome: the endocrine tumor gene *HRPT2* maps to chromosome 1q21–q31. Am J Hum Genet. 56:944–950.
15. **Hobbs MR, Pole AR, Pidwirny GN, et al.** 1999 Hyperparathyroidism-jaw tumor syndrome: the *HRPT2* locus is within a 0.7-cM region on chromosome 1q. Am J Hum Genet. 64:518–525.
16. **Williamson C, Cavaco BM, Jausch A, et al.** 1999 Mapping the gene causing hereditary primary hyperparathyroidism in a Portuguese kindred to chromosome 1q22–q31. J Bone Miner Res. 14:230–239.
17. **Shibata D.** 1994 Extraction of DNA from paraffin-embedded tissue for analysis by polymerase chain reaction: new tricks from an old friend. Hum Pathol. 25:561–563.
18. **Manickam P, Guru SC, Debelenko LV, et al.** 1997 Eighteen new polymorphic markers in the multiple endocrine neoplasia type 1 (*MEN1*) region. Hum Genet. 101:102–108.
19. **Kallioniemi OP, Kallioniemi A, Piper J, et al.** 1994 Optimizing comparative genomic hybridization for analysis of DNA sequence copy number changes in solid tumors. Genes Chromosom Cancer. 10:231–243.
20. **Lloyd SE, Pearce SH, Fisher SE, et al.** 1996 A common molecular basis for three inherited kidney stone disease. Nature. 379:445–449.
21. **Schmidt L, Duh FM, Chen F, et al.** 1997 Germline and somatic mutations in the tyrosine kinase domain of the MET protooncogene in papillary renal carcinomas. Nat Genet. 16:68–73.
22. **Schmidt L, Junker K, Weirich G, et al.** 1998 Two North American families with hereditary papillary renal carcinoma and identical novel mutations in the MET protooncogene. Cancer Res. 58:1719–1722.
23. **Sidhar SK, Clark J, Gill S, et al.** 1996 The t(X;1)(p11.2;q21.2) translocation in papillary renal cell carcinoma fuses a novel gene PRCC to the TFE3 transcription factor gene. Hum Mol Genet. 5:1333–1338.
24. **Weterman MA, Wilbrink M, Geurts van Kessel A.** 1996 Fusion of the transcription factor TFE3 gene to a novel gene, PRCC, in t(X;1)(p11;q21)-positive papillary renal cell carcinomas. Proc Natl Acad Sci USA. 24:15294–15298.
25. **Bergerheim US, Frisk B, Stellan B, Collins VP, Zech L.** 1990 Del(3p)(p13p21) in renal cell adenoma and del(4p)(p14) in bilateral renal cell carcinoma in two unrelated patients with von Hippel-Lindau disease. Cancer Genet Cytogenet. 49:125–131.
26. **The BT, Lindblad K, Hii S, et al.** 1999 Familial testicular cancer: lack of evidence for trinucleotide repeat expansions and association with PKD1 in one family. J Med Genet. 36:348–349.
27. **Zhuang Z, Park WS, Pack S, et al.** 1998 Trisomy 7-harbouring nonrandom duplication of the mutant MET allele in hereditary papillary renal carcinomas. Nat Genet. 20:66–69.